Some Properties of Lysozyme−Lithium Perfluorononanoate Complexes

Alessandro Ciurleo,[†] Stefania Cinelli,[‡] Monia Guidi,[§] Adalberto Bonincontro,[§,#] Giuseppe Onori,[‡,#] and Camillo La Mesa*[,†,#]

Department of Chemistry, La Sapienza University, Rome, Italy; Department of Physics and CEMIN, Perugia University; CNISM-Department of Physics, La Sapienza University, Rome, Italy; and INFM-SOFT CNR Research Centre, La Sapienza University, Rome, Italy

Received June 27, 2006; Revised Manuscript Received September 29, 2006

Mixtures containing lysozyme, LYSO, and a fully fluorinated surfactant, lithium perfluorononanoate, LiPFN, were investigated in a wide range of concentrations and mole ratios. To ensure consistency to the data, a comparison was made, when possible, with the more conventional SDS as surfactant. Molecular solutions, precipitates, and micellar phases have been observed. The region of existence for each phase depends on the LiPFN/LYSO mole ratios, *r*, and was determined by different experimental methods. Optical absorbance, CD, ^{19}F NMR, viscosity, electrical conductivity, and dielectric relaxation methods were used. Some methods give information on the protein conformation, others on the state of the surfactant or on the collective system properties, respectively. Addition of LiPFN gives rise to a solution, a poly phase dispersion (at low surfactant to protein ratios) and to a micelle-mediated redissolution of the precipitates. Concomitant to the above macroscopic properties, peculiar effects in the state of LYSO are observed. Low amounts of surfactant reduce significantly the amount of α-helix in favor of the β-sheet conformation of the protein. The former is almost completely regained once micelle-assisted redissolution of the complex occurs. The tertiary structure of the protein, conversely, is lost at low surfactant content and never recovered. Such evidence suggests the occurrence of a molten globule conformation for LYSO in micellar media.

Introduction

A large body of experimental evidence on the interactions between proteins and surfactants is currently available. Studies reported so far deal with the binding of sodium dodecylsulfate, SDS, to bovine serum albumin, BSA, or lysozyme, LYSO.[1,2] Besides their relevance in fundamental investigation, such studies are also important in biochemical separation, drug delivery, cosmetics, and detergents.[3,4] Investigation of SDS binding to proteins yields complex results, indicating several levels of affinity between the two components. Generally, specific noncooperative binding occurs at low surfactant content and is followed by nonspecific and cooperative effects at high concentrations.[5] The formation of precipitates is observed upon addition of small quantities of surfactant, whereas redissolution needs large amounts of the amphiphilic species.[6,7] This complex behavior is due to a delicate balance between protein−surfactant and surfactant−surfactant interactions.

Proteins and surfactants share the property of having charged groups and large hydrophobic portions. This peculiarity implies that the interactions between surfactants and proteins are intrinsically complex processes, involving the overlapping of different types of molecular forces (vdW, hydrophobic, and electrostatic). The resulting interactions have a pronounced effect on protein−surfactant systems, (PSS), and on the structure of their complexes, as well. Perhaps, it is not easy to ascertain which contribution controls the rich polymorphic behavior occurring in PSS.

Turro recently summarized the different models proposed so far to describe the formation of BSA−SDS complexes.[8] The "necklace and bead" model assumes that the complexes are composed by small micelles with uncoiled BSA units wrapped around and has strong experimental support.[9,10] Different opinions exist on LYSO conformation in LYSO−SDS complexes. Some authors observed the unfolding of the protein native structure upon SDS binding, and others stated that lysozyme does not unfold.[11−13]

Although studies on the stability of protein−surfactant complexes (PSC)[14] and on surfactant binding to proteins[15] are well established, the microstructure of PSC is not yet fully understood. The determination of the structural state of proteins interacting with surfactant molecules in different self-aggregation states is, thus, a really important task.

To get information on the interplay between hydrophobic and electrostatic contributions to the stability of PSC and to clarify still open questions on their microstructure, a systematic investigation on a system composed by water, a globular protein, and a fully fluorinated surfactant was performed. Replacement of protons with fluorine atoms increases the lipophilic character of the surfactant alkyl chains and influences the interactions with polymers[16] and, very presumably, with proteins. The resulting interactions are mostly controlled by electrostatic contributions. Hydrophobic interactions between the apolar regions of the protein and the fluorinated surfactants, conversely, can be ruled out.[17] Hydrophobic contributions, perhaps, are relevant in fluorocarbon−fluorocarbon interactions.[18]

Fluorinated molecules (such as fluoro-alcohols, for instance)[19] are considered protein stabilizers. Not much is known, however, on the effect that fluorinated surfactants have on protein stability and conformation. This is surprising, in view of the extensive

* Corresponding author. E-mail address: camillo.lamesa@uniroma1.it.
† Department of Chemistry, La Sapienza University.
‡ Perugia University.
§ CNISM-Department of Physics, La Sapienza University.
# INFM-SOFT CNR Research Centre, La Sapienza University.

10.1021/bm060609d CCC: $37.00
Published on Web 12/23/2006

use of fluorine-containing products in pharmaceutical formulations and in biomedical applications (such as blood substitutes for transfusions),[20] that demand a deep knowledge on protein−fluorocarbon interactions.

In previous work, the phase behavior of LYSO and lithium perfluorononanoate, LiPFN, in water was investigated.[17,21] Different phases and multiphase regions were observed. In particular, a two-phase region, when the solution coexists with a precipitate, follows a tiny solution phase, L^0, occurring at low protein and LiPFN content. Higher surfactant concentrations redissolve the poorly soluble LYSO−LiPFN complexes.

The present work attempts to clarify previous studies and focuses on conformational changes, when the formation of PSC occurs. To define how much surfactant is required to saturate the protein and to clarify the structure of the complexes are, in fact, questions of fundamental interest. The complexes and gels formed at high surfactant to protein ratios had received major attention,[22,23] although their precise structure is not well-known.[24]

In our opinion, ad hoc techniques, such as CD, ^{19}F NMR, dielectric relaxation, and ancillary methods may fully characterize the complexes formed in the water−LYSO−LiPFN system. Use of fluorinated species, for instance, avoids the overlapping of the ^{1}H NMR signals of the protein with those of the surfactant. Other methods focus exclusively on protein conformation; selected ones, finally, refer to the overall system behavior. In this way a comprehensive view of the system properties is at hand.

Some biochemical consequences inherent to the observed behavior shall be examined. In particular, denaturation and partial renaturation of the protein, with subsequent formation of a molten globule conformation, are discussed. Effects pertinent to the molten globule conformation of proteins in micellar solutions are relevant in most biochemical separation technologies.

Experimental Section

Materials. Chicken egg lysozyme, LYSO (fract. V, Sigma), was dissolved in 0.15 M NaCl, dialyzed against water, recovered, lyophilized, and dried over P_2O_5. Its purity was controlled by density and viscosity measurements of its aqueous solutions.[25,26]

Buffers were avoided, since the solution pH is always in the range 6.4−6.6, and practically independent of added LYSO and LiPFN (or SDS). Furthermore, addition of buffers implies counterion binding onto the polar groups of the protein and has a significant effect on its effective charge and on the double layer thickness around LYSO and/or the micellar aggregates. In case of buffer-containing systems, finally, counterion exchange processes should be considered. In the experimental pH conditions used in the present work, LYSO has eight positive charges in excess.[6]

Lithium perfluorononanoate, LiPFN, was obtained by titrating the corresponding acid, Riedel, with LiOH; the resulting salt was purified as in previous work.[27] The conductometric determination of the critical micellar concentration, CMC, at 25.00 °C, was used as a purity criterion and is in good agreement with previous findings.[28]

Water was doubly distilled in a Pyrex all-glass apparatus over alkaline $KMnO_4$. The ionic conductivity of freshly distilled water, χ, is in the range 0.7−1.0 μS cm^{-1} at 25.00 °C.

The mixtures were prepared by weight and equilibrated at room temperature for 1 day. D_2O, Merck 99.5% isotopic enrichment, was used on a mole fraction basis. Depending on the investigated region, the mole ratios are r in [LiPFN/LYSO] molecular solutions, and r^{-1} in [LYSO/LiPFN] micellar ones, respectively.

Methods. *CD Measurements.* The experiments were performed on a JASCO J-810 spectropolarimeter, at 25.0 ± 0.1 °C. In far-UV conditions (190−240 nm), cells with 0.1 cm optical length were used. The protein concentration was 0.19 mg/g (12×10^{-6} molal), unless otherwise stated. In all samples the turbidity is small and CD spectra are null out of the absorbance band(s). This allowed performing experiments in the far-UV on the same samples used in turbidity measurements. In the near-UV region (240−320 nm) cells with 1.0 cm optical length were used. CD results are expressed as mean residue ellipticity, θ (deg cm^2 dmol^{-1}).

UV-vis Absorbance. Absorption spectra were recorded by a Jasco V-570 spectrophotometer, working between 190 and 680 nm, at 25.0 ± 0.1 °C.[29] The cell path length is 0.1 cm. The absorbance of the solutions, A, was measured at 340 nm.

^{19}F NMR. An INOVA 300 MHz unit, Varian, was used to measure the ^{19}F spectra at 300 K, according to previously reported procedures.[16] The assignment of the resonance lines has been reported in previous work.[21] T_2 values (in Hz) were measured at the half-height peak. NMR measurements were performed after adding LYSO. The protein−surfactant solutions were allowed to stay until the systems had reached the equilibrium conditions. In all experiments the systems did not show inhomogeneities or macroscopic phase separation.

Ionic Conductivity. A 6425 Wayne-Kerr impedance bridge was used. The conductivity cell was located in an oil bath, working at a temperature, T, of 25.000 ± 0.003 °C. Known amounts of water−LYSO−LiPFN solutions were added to aqueous LiPFN by a weight burette, under mild stirring. Plots are reported as χ (mS cm^{-1}) versus the mole ratio between the two components.

Viscosity. Ubbelohde viscometers, Schott Geräte, have flow times in the range 2−300 s (to minimize spurious kinetic effects) and were located in a water bath, at 25.00 ± 0.01 °C. The accuracy on flow times, t, was ≈0.3 s and each datum the average of five independent runs. Viscosity findings ($\eta_{rel} = t\rho/t^\circ\rho^\circ$) were taken relative to the surfactant, or the protein solution, and corrected for the respective densities. The solution, ρ, and solvent, ρ° (g cm^{-3}), densities were measured by a DMA 60 vibration densimeter (Anton Paar), equipped with a Heto thermostatic unit.

Dielectric Relaxation. The dielectric permittivity, ϵ', and loss, ϵ'', were measured by a HP 4291-A computer-controlled impedance analyzer, in the range 10^6−10^9 Hz. The cell was realized with the termination of a coaxial line, filled with the solution.[30] The temperature was 25.0 ± 0.1 °C. The measured reflection coefficient and phase angle at the interface with the sample were converted into real, ϵ', and imaginary, ϵ'', components of the complex dielectric constant, ϵ^* ($\epsilon^* = \epsilon' - j\epsilon''$). An interpolation method, based on the comparison with solutions of conductivity close to the investigated mixtures, was used.[31] The relaxing part of the dielectric loss, ϵ_d'', was obtained by subtracting the conductive contribution, $(\chi/\epsilon_o 2\pi f)$, from the experimental results. There f is the frequency of the applied electric field and ϵ_o the dielectric constant of vacuum. The errors on ϵ' values are ±1.0%, those on ϵ'' ±3.0%.

Results and Discussion

In mixtures containing water, proteins, and surfactants, a rich phase behavior is usually observed, with formation of solutions, precipitates, and gels.[6,32] In dilute regimes of the water−LYSO−LiPFN system, the following regions are found:[21]

(i) A molecular solution, containing tiny amounts of surfactant and protein;

(ii) A wide multiphase area, where protein−surfactant complexes precipitate. They

may not have the same stoichiometry at all concentrations;

(iii) A micellar solution, when the protein−surfactant complexes are redissolved.

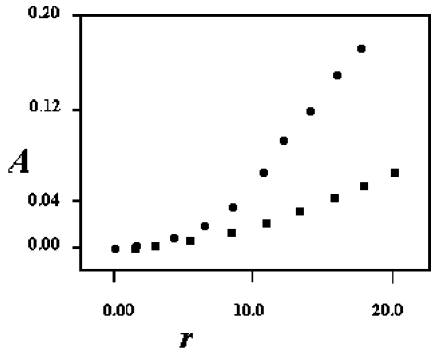

Figure 1. Comparison of optical absorbance data, *A*, at 340 nm and 25.0 °C, of 12 μmol kg^{-1} LYSO aqueous mixture as a function of added amphiphile. Data are reported as surfactant to polymer ratio, *r*, for SDS (●), and LiPFN containing systems (■).

The methods used in this work offer the opportunity to focus onto properties peculiar to a given species; CD on protein conformation, for instance, and ^{19}F NMR on the surfactant. The results obtained from the different experimental methods are reported separately below.

Turbidity and CD. This work takes up a problem with bearing on protein−surfactant interactions and more specifically on fluorinated surfactant−protein interaction. The reasons why a fluorinated surfactant has been chosen arise from the need to clarify previous work[21] and also from the difficulty to perform CD and NMR experiments with the more conventional SDS surfactant. The formation of aggregates in the SDS−LYSO system may imply difficulties in the elaboration of optical experiments. Solutions containing the latter species, in fact, are much more turbid than the LiPFN-containing ones. This is presumably due to a much faster aggregation, with formation of clusters and/or to differences in the refractive index of SDS-containing systems with respect to LiPFN-containing systems. To our knowledge, however, no such comparison has been reported in the literature.

This is the reason why the behavior relative to the two surfactants can be compared only in highly dilute regimes, Figure 1. In both systems, turbidity increases for $r > 8$ (which is the number of positive charges in excess of lysozyme). However, in the SDS−LYSO system the scattering is much higher and, unexpectedly, the nucleation and phase separation kinetics occur over much shorter time scales. This effect can be due to the more significant overlapping of hydrophobic and electrostatic contributions in mixtures containing SDS. The behavior reported in Figure 1 indicates some specificity in binding and suggests that SDS has a stronger effect on the nucleation of protein−surfactant complexes. This is not an easy task to solve, since SDS and LiPFN solutions may have different refractive indexes.

Turbidity data for the LiPFN−LYSO system are reported in Figure 2, where three concentration regimes can be defined when the protein content is kept constant. The solution turbidity increases when the mole ratio *r* is in the 0−50 range and reaches a saturation threshold thereafter. Above $r = 18$ (the number of LYSO cationic sites) the turbidity steeply increases. Full saturation and constant turbidity are achieved for *r* values close to 40. The turbidity remains nearly constant up to 8.0 mmol kg^{-1} LiPFN, close to theCMC,[28] and rapidly levels off above that value.

Some general trends clearly emerge from such experiments, but it is not easy getting quantitative information from optical absorbance only. CD studies in far-UV conditions (in the range 190−240 nm) assess quantitatively the secondary structure of

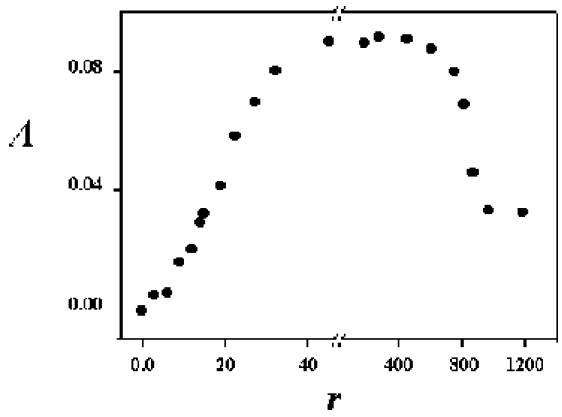

Figure 2. Optical absorbance, *A*, at 340 nm and 25.0 °C, vs the mole ratio [LiPFN/LYSO], indicated as *r*. The mother solution contains 12 μmol kg^{-1} LYSO.

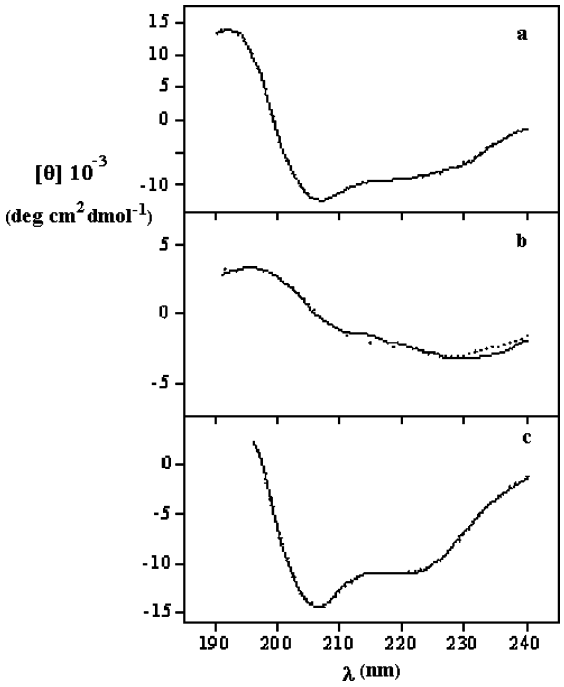

Figure 3. (a) Far-UV CD spectra of LYSO (12 μmol kg^{-1}) in water, at 25.0 °C, reported as θ (deg cm^2 dmol^{-1}) vs λ (nm). The same system with (b) 0.54 mmol kg^{-1} LiPFN added, and (c) with 10.0 mmol kg^{-1} LiPFN added. The full lines represent the experimental values; the dotted ones were obtained by a *CONTIN* algorithm.

the protein, when those in the near UV range (240−320 nm) are a probe to investigate the tertiary structure of the protein. The differential scattering of left and right circularly polarized light gives an important contribution to the CD spectra of biomolecules, and it is expected to be significant when the scattering contribution to the apparent CD is measured outside the absorption bands of the protein. In the LiPFN−LYSO system, however, such signal is null, while it is significant in the SDS−LYSO system.

Important results concerning the changes in the secondary and tertiary structures of the protein upon interactions with increasing amounts of the surfactant are given in Figures 3, 4 and 5. Unfortunately, an analysis of CD spectra in the SDS−LYSO system did not give significant information on protein conformation, because of the relevant solution scattering.[33]

CD spectra relative to pure LYSO and to LiPFN−LYSO mixtures are reported in Figure 3. A transition in the secondary structure of LYSO was inferred as *r* varied in the 0−50 range.

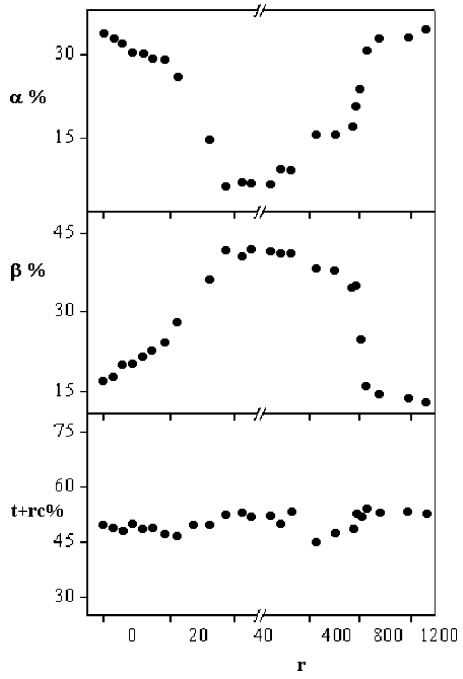

Figure 4. The percentage of α-helix, up, β-sheet, medium, and [turn + r.c.] conformations, down, of LYSO as a function of *r*, at 25.0 °C. The points are accurate to ±1.0%.

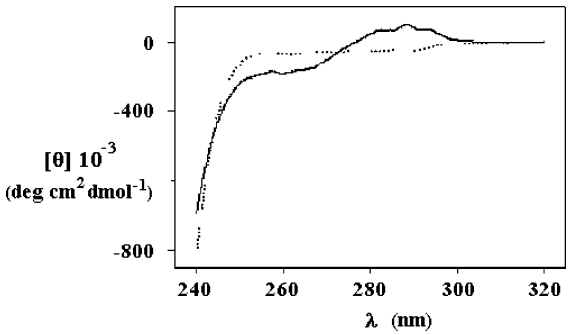

Figure 5. Near-UV CD spectra, reported as θ (deg cm^2 dmol^{-1}) vs λ (nm) of solutions containing 12 μmol kg^{-1} LYSO with 0.22 mmol kg^{-1} LiPFN, full line, and with 10.0 mmol kg^{-1} LiPFN, dotted line, at 25.0 °C.

The analysis of CD spectra was elaborated by a CONTIN algorithm.[34] For $r = 0$ the amount of α-helix is 0.34 and that of β-sheet 0.17; the remaining is the [turn + random coil] term, (Figure 3a). For $r = 45$ the amount of α-helix drops to 0.07, and that of the β-sheet increases to 0.41 (Figure 3b). At concentrations well above the CMC, for very high LiPFN−LYSO ratios (Figure 3c), the protein recovers its secondary structure and is characterized by an amount of α-helix close to 0.34, whereas the β-sheet contribution decreases to 0.13.

In Figure 4 the relative weight of each conformation as a function of *r* is reported. For $r > 18$, the changes in slope become sharper and level off when $r \approx 40$. Addition of LiPFN, at concentrations above the CMC, promotes the $\beta \rightarrow \alpha$ transition and LYSO conformation is again similar to the native one. The [turn + random coil] fraction slightly increases in the whole range of *r* values. The good correspondence between turbidity (Figure 2) and the relative amount of α or β conformation (Figure 4) as a function of *r* indicates that the aggregation increases as the conformational transition takes place. The association between LYSO and LiPFN below the CMC is largely different compared to that above it. In the latter region, in fact, the protein almost completely retains its secondary structure.

Far-UV CD data indicate strong correlation between the relative amount of β-structure and the aggregation extent. Aggregation, presumably, involves the formation of folded intermediates, apt to self-associate because of a partial exposure of the protein hydrophobic core.[35] On this regard, it was recently demonstrated that LYSO forms amyloidal fibrils and that a structural state of the protein rich in β-sheet is a prerequisite for its aggregation.[36]

Further information on protein structure is obtained by CD in the 240−320 nm range. This is a fingerprint region, as to the tertiary structure of LYSO is concerned, and gives important information on the molten globule state of proteins.[37] Signals in the near-UV region are much weaker than in the far-UV region, and use of cells with high optical length is required. The spurious contributions due to the differential scattering are negligible for $r \leq 18$, and the spectra do not show significant changes in the tertiary structure of LYSO up to this concentration ratio.

The sharp rise in turbidity for $r > 18$ does not allow measurement of a spectrum; measurements are possible only when micelle-assisted redissolution of the complexes occurs. In this region the spectra are flat (Figure 5), showing a complete loss of the tertiary structure of the protein. In particular, the signal at 280 nm, peculiar to the tertiary structure of the protein, disappears.

CD data indicate that the secondary structure of LYSO is significantly retained, whereas the tertiary structure is irreversibly lost. This behavior is typical of a molten globule conformation. The biological significance of such state is relevant in protein translocation across membranes,[38] since the transition to molten globule increases the hydrophobic character of proteins and favors their insertion into cells.

The studies reported above are essentially oriented to clarify the interactions between LYSO and the surfactant in molecular form. Those in the following section, conversely, are oriented to clarify the interactions between the protein and micellar aggregates.

NMR. Measurements were performed by adding progressive amounts of LYSO to micellar LiPFN solutions. This procedure allows the collection of information on changes in surfactant aggregation modes, due to protein binding onto micelles. At high LYSO/LiPFN mole ratios, the signals of most CF_2 units overlap, and a complete resolution of the state of fluorocarbon chains is not possible and makes questionable a proper assignment of the processes occurring in such mixtures, Figure 6a. Fortunately, the triplet ascribed to the terminal CF_3 and the signal of the CF_2 unit close to the polar head group are well separated from the other signals. Thus, modifications in the behavior relative to the micelle interior and to its outer surface, respectively, can be investigated. In particular, the chemical shifts and relaxation times relative to the outer CF_2 units systematically change upon addition of LYSO, while the former do not. From the chemical shifts it is clear that the fluorine atoms located close to the interface of the micelles are more influenced by the presence of LYSO. This does not univocally prove that LYSO binds onto the micelles, even if ionic conductivity and dielectric relaxation show that this hypothesis is reasonable. In NMR the contributions responsible for the line broadening are due to the rotational motions of the aggregates as a whole (including bound LYSO) and to the chain motion with respect to the binding site. In this hypothesis, the groups more involved in the spectral width modifications are the ones closer to the protein. The behavior reported in Figure 6b and 6c is a clear indication that binding is related to surface

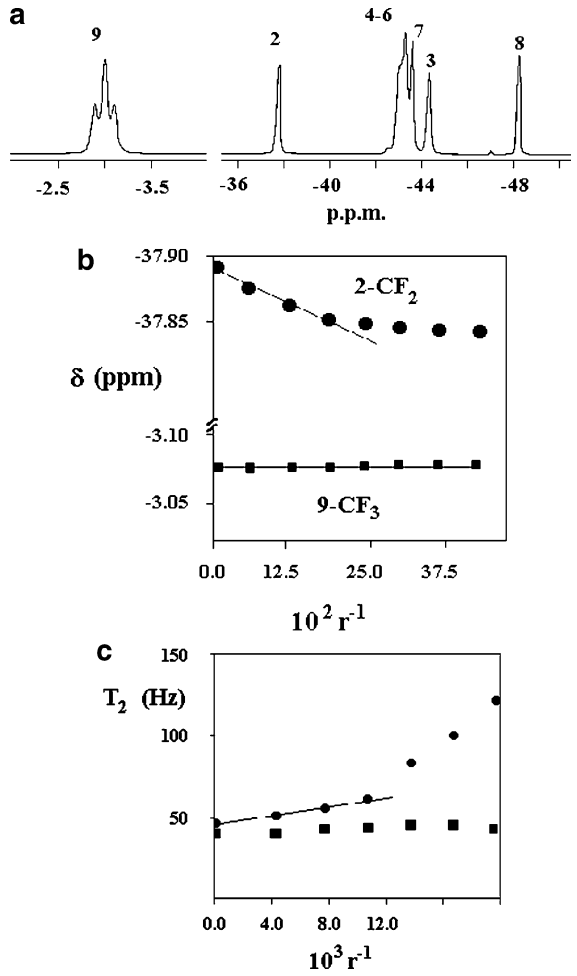

Figure 6. (a) ^{19}F NMR spectra of a 690 μmol kg^{-1} LYSO in 63.0 mmol kg^{-1} LiPFN solution, at 300 K. Numbers indicate the position of the CF_2 (CF_3) groups with respect to the polar head. The CF_3 triplet, on the left-hand side, is enlarged. (b) Dependence of the chemical shift, δ, in ppm, of signals 2 (●) and 9 (■) as a function of the mole ratio [LYSO/LiPFN], r^{-1}, for solutions containing 31.5 mmol kg^{-1} LiPFN, and progressive amounts of protein, at 25.0 °C. (c) T_2 values (in Hz), measured at the half-height signal width, vs r^{-1}, for the same mixtures, at 25.0 °C. The values are relative to signals 2 (●) and 9 (■).

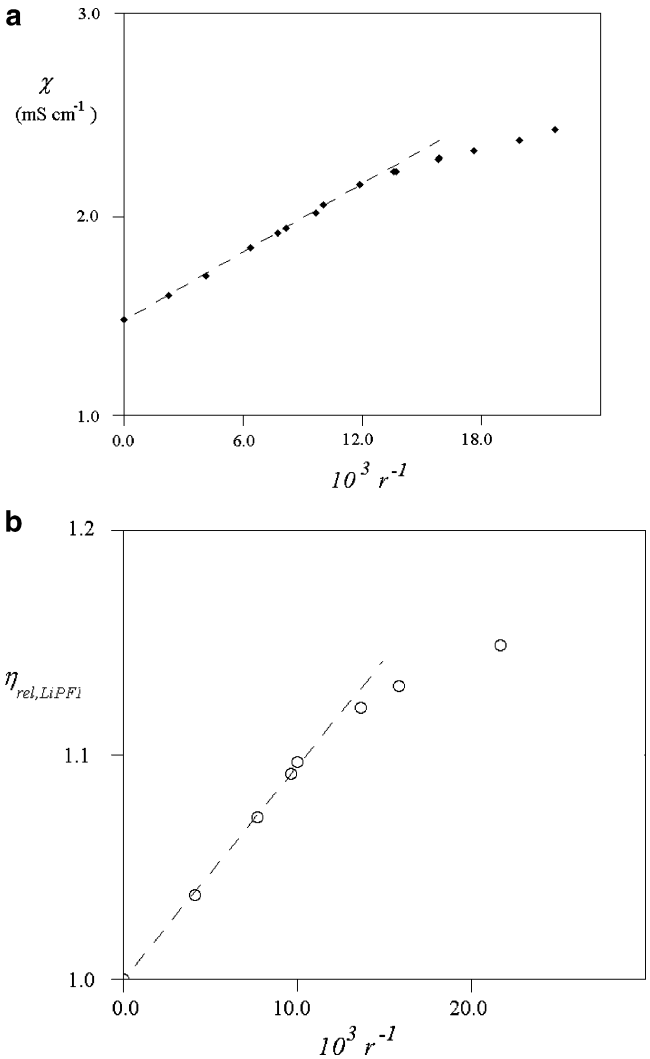

Figure 7. The ionic conductivity, χ (mS cm^{-1}), (●) up, and, the relative viscosity, $\eta_{rel,LiPFN}$, (○) down, vs r^{-1}, in micellar solution containing progressive amounts of LYSO, at 25.00 °C. The solvent contains 32.0 mmol kg^{-1} LiPFN.

adsorption of LYSO onto micelles. Binding is progressive and becomes significant for large concentrations of protein. It can be inferred, for instance, by the significant changes in slope observed in T_2 values versus r^{-1} plots. It is possible that some terminal CF_3 groups are exposed to water, as, indeed, holds for hydrocarbon surfactants. Perhaps fluorinated chains are by far more rigid than hydrocarbon-based chains and exposure to water would imply a significant conformational energy contribution. The changes in slope observed in the signal due to the CF_2 unit close to the polar head group occur at the same ratios observed in conductivity and viscosity results.

Transport Properties. In the micellar regime the concentration of LYSO−LiPFN complex(es) was modulated by adding the protein. Some changes in transport properties are observed, Figure 7. The hydrodynamic volume of the LYSO−micelle complexes increases in proportion to protein content, up to saturation, with formation, presumably, of anisometric aggregates. When added protein binds onto micelles, lithium ions are partly replaced by LYSO and released, with consequent increase in the overall ionic mobility of the system. The changes in slope in Figure 7 are reasonably ascribed to the completion of protein binding onto micelles. It is worth mentioning that the observed changes in slope occur at the same values as those reported in the NMR section.

Dielectric Relaxation. Dielectric relaxation processes were modulated by adding the protein to surfactant solutions, at concentrations well above the CMC. Some spectra are reported in Figure 8. These processes are ascribed to the polarization mechanisms of counterions around charged aggregates and change significantly when the protein binds onto micelles. The data were fitted according to the Cole−Cole equation,[39] as

$$\epsilon(\omega) = \epsilon_\infty + \left[\frac{\Delta\epsilon}{1 + (j\omega\tau)^{(1-\alpha)}}\right] \qquad (1)$$

where j is $\sqrt{-1}$, $\Delta\epsilon$ the dielectric increment with respect to the high-frequency value, ϵ_∞, τ the relaxation time, ω the measuring angular frequency, and α an empirical parameter related to the spreading of relaxation times. The $\Delta\epsilon$, α, and f_r ($f_r = 1/2\pi\tau$) values obtained by eq 1 are reported in Table 1, and the relaxation times, τ, are drawn in Figure 9 as a function of r^{-1}. The figure shows a change in slope at the same value of r^{-1} obtained by the other techniques. The data indicate that protein binding has occurred. Below the inflection point in Figure 9 no occurrence of more relaxation processes is observed, and the presence of dynamic modes due to the free protein (at frequences close to 9 MHz) is negligible.

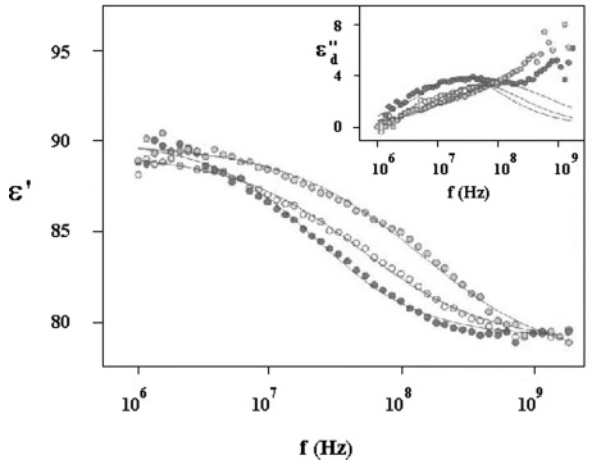

Figure 8. Dielectric relaxation spectra in LYSO-containing LiPFN 32.0 mmol kg^{-1} micellar solutions, at 25.0 °C, reported as ϵ' vs f (Hz) plots. Data refer to the following [LYSO/LiPFN] mole ratios: 3.0×10^{-3} (middle gray), 7.5×10^{-3} (light gray), and 1.9×10^{-2} (black) r^{-1}. In the inset the plots of ϵ_d'' vs f (Hz) are reported. At high frequencies, the relaxing polarization modes due to the solvent can be observed.

Table 1. The [LYS/LiPFN] Mole Ratio, r^{-1}, the Dielectric Increment, $\Delta\epsilon$, the Relaxation Frequency, f_r, and the α Parameter in eq 1, at 25.0 °C[a]

10_3 r^{-1}	$\Delta\epsilon$	f_r (MHz)	α
0.0	12.7 ± 0.9	250 ± 20	0.35 ± 0.04
1.5	12.3 ± 0.6	193 ± 18	0.33 ± 0.03
3.0	12.4 ± 0.8	138 ± 13	0.36 ± 0.04
4.2	12.6 ± 0.6	112 ± 12	0.36 ± 0.04
6.0	12.2 ± 0.6	81 ± 8	0.34 ± 0.04
7.5	11.5 ± 0.6	52 ± 5	0.38 ± 0.04
11.3	12.5 ± 0.6	32 ± 3	0.37 ± 0.04
15.0	11.9 ± 0.6	27 ± 3	0.30 ± 0.04
18.9	11.0 ± 0.5	23 ± 2	0.26 ± 0.04
22.5	11.1 ± 0.7	17 ± 2	0.41 ± 0.05
26.4	11.3 ± 0.9	14 ± 2	0.36 ± 0.t06
30.0	9.9 ± 0.5	12 ± 1	0.26 ± 0.04
37.5	9.1 ± 08	12 ± 2	0.28 ± 0.06

[a] The mother solution contains 32.0 mmol kg^{-1} of surfactant.

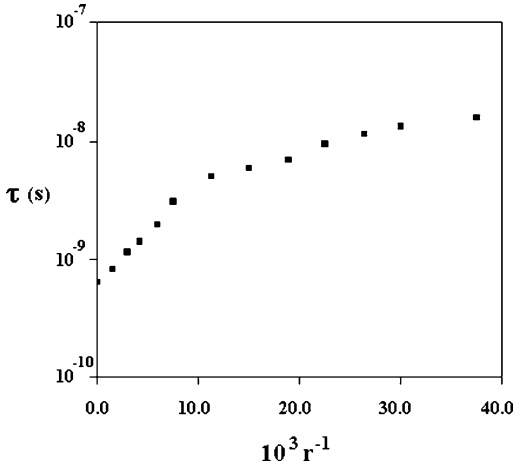

Figure 9. Dependence of the dielectric relaxation time, τ (s), in logarithmic scale, on r^{-1}, at 25.0 °C. The mother LiPFN solution contains 32.0 mmol kg^{-1} of surfactant.

The dielectric behavior can be rationalized in terms of modifications in the micelle surface charge density, due to interactions with LYSO. This is reflected in significant modifications in the double layer thickness around micelles and can be quantified in terms of the models reported by Grosse[40,41] and, independently, by Pottel.[42] The former introduced a model for the polarization of counterions and extended it to particles of arbitrary charge. Pottel, conversely, developed the empirical spectral functions, to get information on the degree of dissociation, the effective size of the aggregates, and the mobility of counter-ions not firmly bound.

The dielectric relaxation times in Figure 9 were related to the aggregate size, according to the following relation,[42]

$$\tau = \left[\frac{R^2}{2D_{\mathrm{Li}}^{\circ}}\right] \qquad (2)$$

where D°_{Li} is the limiting self-diffusion coefficient of lithium ions in water and R is the radius of the PS complexes (including the thickness of the double layer). The average radius of the complex can be evaluated, assuming D°_{Li} in eq 2 to be 1.3×10^{-9} m^2 s^{-1}.[43] Variations in τ (and in R) values are significant above and below the change in slope in Figure 9. Above that limit, the mixtures contain, presumably, protein−micelle complexes, small amounts of free micelles, and free LYSO. In these systems molecular surfactant species and lithium ions do also occur, but they are not responsible for any dielectric relaxation process.

From a purely phenomenological viewpoint, the results indicate that the average radius of the LYSO−LiPFN$_{\mathrm{mic}}$ complexes, evaluated by eq 2, is about three times that of free micelles. The charge density of the complex is also quite different with respect to the mother species (free protein and free micelles), and the double layer thickness changes accordingly. This behavior is reflected by the decrease in $\Delta\epsilon$ values.

The dielectric results can be modeled in terms of equivalent charged spheres. If such a hypothesis holds, LYSO interacts with about 100 fluorinated ions (corresponding to four spherical micelles, if their aggregation numbers do not change). Similar conclusions on the stoichiometry are inferred by transport and NMR methods, indicating significant changes in slope of the corresponding properties at the same mole ratios. Modeling the dielectric response of all objects (protein, micelles, and complexes) in terms of charged spheres, indicates that the complexes have lower charge density compared to the starting species. Close to the inflection point in Figure 9 the data elaboration by eq 2 indicates that the radius of the complex(es) is about 5 nm, including the double layer thickness. This value is reasonable if compared to the hydrodynamic radius of micelles and LYSO (about 2 nm each).

In the region where LYSO−micelle complexes exist, the following conclusions can be drawn. The amount of protein in excess is not consistent with the dielectric relaxation amplitude expected for the free protein. Presumably, LYSO is still involved in binding onto micelles, although at a reduced rate, because of the high steric hindrance toward further binding stages. In other words, LYSO finds difficulties in binding onto partially neutralized micelles, with subsequent effects on the dynamics of the process.

Conclusions

Information inferred from different experimental methods, chosen to account for the behavior of the protein (CD), of the surfactant (^{19}F NMR), and the collective properties of LYSO−LiPFN complexes (dielectric relaxation), were discussed. As a consequence of protein−surfactant interaction, a quite complex behavior has been observed.

As the relative amounts of α and β conformations show, the protein retains its native structure for low LiPFN/LYSO mole ratios. Once binding onto LYSO starts to occur and the surfactant concentration increases, the amount of α conformation drops and, in the same time, the tertiary structure is lost. It will never be recovered, whereas the amount of α-helix conformation increases again, after the redissolution of the precipitate by LiPFN micelles. The above behavior is concomitant with an increase in the size of the micellar aggregates. According to both dielectric relaxation and ^{19}F NMR, a surface binding process occurs.

Surfactant−surfactant interactions, responsible for the stability of micelles, are more significant in fluorocarbons than in hydrocarbon surfactants. Fluorocarbon chains are quite bulky and, presumably, do not enter into the hydrophobic pockets of the protein. More presumably, binding is essentially due to the interactions between the charged groups facing outward from the protein and the surfactant ions or micelles (depending on concentration). Saturation of the binding sites favors protein denaturation and increases its hydrophobic character.[44,45]

In vivo, protein aggregation occurs in a wide range of experimental conditions, some of which are similar to those observed in low concentration protein−surfactant systems. In some cases, the aggregation leads to a perturbation of the biological functions, with serious physiological consequences, as in the formation of cataracts in the eye lenses or in amyloidal fibrils, associated with Alzheimer and other neurological diseases.[46,47]

Conversely, the binding of LYSO to micelles mimics the conformational changes, with changes in the tertiary structure, occurring when proteins are inserted into the double layers of biological membranes. It should be interesting to clarify whether the same behavior occurs when natural and/or synthetic vesicles replace micelles.

Acknowledgment. This work was partly supported by CEMIN (Centro di Eccellenza Materiali Innovativi Nanostrutturati). The research was performed under the auspices of the European Community, by a COST D-35 Action Project on Interfacial Chemistry and Catalysis, 2006−2010. Special thanks are due to Anna Laura Segre, Institute of Chemical Methodologies, CNR, for help, technical assistance in measuring ^{19}F NMR spectra and fruitful discussions on some aspects of the manuscript.

References and Notes

(1) Zanette, D.; Lima, C. F.; Ruza, A. A.; Belarmino, A. T. N.; Santos, S. de F.; Frescura, V. L. A.; Marconi, D. M. O.; Froehner, S. J. *Colloids Surf. A.* **1999**, *147*, 89.
(2) Chatterjee, A.; Moulik, S. P.; Majhi, P. R., Sanyal, S. K. *Biophys. Chem.* **2002**, *98*, 313.
(3) Goddard, E. D. In *Interactions of Surfactants with Polymers and Proteins*; Goddard, E. D., Ananthapadmanabhan, K. P., Eds.; CRC Press: Boca Raton, FL, 1993; p 395.
(4) Rodenhiser, A. P.; Kwak, J. C. T. In *Polymer-Surfactant Systems*; Surfactant Science Series, M. Dekker: New York, 1998; p 1.
(5) Chronakis, I. S.; Fredholm, A.; Triantafyllou, A. O.; Oste, R. *Colloids Surf. B*: *Biointerfaces* **2004**, *35*, 175.
(6) Moren, A. K.; Khan, A. *Langmuir*, **1995**, *11*, 3636. Moren, A. K.; Khan, A. *Langmuir* **1998**, *14*, 6818, and references therein.
(7) Valstar, A.; Vasilescu, M.; Vigouroux, C.; Stilbs, P.; Almgren, M., *Langmuir* **2001**, *17*, 3208. Valstar, A.; Almgren, M.; Brown, W.; Vasilescu, M. *Langmuir* **2000**, *16*, 922. Vasilescu, M.; Angelescu, D.; Almgren, M. *Langmuir* **1999,** *15*, 2635. Valstar, A.; Brown, W.; Almgren, M. *Langmuir* **1999**, *15*, 2366.
(8) Turro, N. J.; Lei, X-G.; Ananthapadmanabhan, K. P.; Aronson, M. *Langmuir* **1995**, *11*, 2525.
(9) Guo, X. H.; Zhao, N. M.; Chen, S. H.; Texeira, J. *Biopolymers* **1990**, *29*, 335.
(10) Shirahama, K. In *Polymer-Surfactant Systems*; Surfactant Science Series, M. Dekker: New York, 1998; p 143.
(11) Jones, M. N.; Prieto, G.; del Rio, J. M.; Sarmiento, F. *J. Chem. Soc. Faraday Trans.* **1995**, *91*, 2805. Jones, M. N.; Prieto, G.; del Rio, J. M.; Sarmiento, F. *Biochem. Soc. Trans.* **1984**, *12*, 625.
(12) Jones, M. N. *Chem. Soc. Rev.* **1992**, *21*, 127.
(13) Takeda, K.; Iba, A.; Shirahama, K. *Bull. Chem. Soc. Jpn.* **1982**, *55*, 985.
(14) Murakami, K. *Langmuir* **1999**, *15*, 4270.
(15) Kujawa, P.; Liu, R. C. W.; Winnik, F. M. *J. Phys. Chem. B* **2002**, *106*, 5578.
(16) Segre, A. L.; Proietti, N.; Sesta, B.; D'Aprano, A.; Amato, M. E. *J. Phys. Chem. B* **1998**, *102*, 10248.
(17) Palacios, A. C.; Sarnthein-Graf, C.; La Mesa, C. *Colloids Surf. A* **2003**, *228*, 25.
(18) Shinoda, K.; Nomura, T. *J. Phys. Chem.* **1980**, *84*, 365.
(19) Sonnichsen, F. D.; van Eick, J. E.; Hodges, R. S.; Sykes, B. D. *Biochemistry* **1992**, *31*, 8790.
(20) Clark, L. C., Jr.; Hoffmann, R. E; Davis, S. L. *Biomater., Artif. Cells Immobilization Biotechnol.* **1992**, *20*, 1085.
(21) Sesta, B.; Gente, G.; Iovino, A.; Laureti, F.; Michiotti, P.; Paiusco, O.; Palacios, A. C.; Persi, L.; Princi, A.; Sallustio, S.; Sarnthein-Graf, C.; Capalbi, A.; La Mesa, C. *J. Phys. Chem. B* **2004**, *108*, 3036.
(22) Roversi, M.; La Mesa, C. *J. Colloid Interface Sci.* **2005**, *284*, 470.
(23) Goddard, E. D. *Colloids Surf.* **1986**, *19*, 255, 301.
(24) La Mesa, C. *J. Colloid Interface Sci.* **2005**, *286*, 148.
(25) Zielenkiewicz, A. *J. Therm. Anal. Calor.* **2001**, *65*, 467.
(26) Monkos, K. *Biochim. Biophys. Acta, Protein Struct. Mol. Enzymol.* **1997**, *1339*, 304.
(27) La Mesa, C.; Sesta, B. *J. Phys. Chem.* **1987**, *91*, 1450.
(28) D'Aprano, A.; Sesta, B.; Proietti, N.; Mauro, V. *J. Solution Chem.* **1997**, *26*, 649.
(29) Bonincontro, A.; Cinelli, S.; Comaschi, T.; Onori, G. *Phys. Chem. Chem. Phys.* **2004**, *6*, 1039.
(30) Bonincontro, A.; Briganti, G.; Giansanti, A.; Pedone, F.; Risuleo, G. *Colloids Surf. B.* **1996**, *6*, 219.
(31) Athey, T. W.; Stuckly, M. A.; Stuckly, S. S. *IEEE Trans. MTT* **1982**, *30*, 82.
(32) Moren, A. K.; Khan, A. *J. Colloid Interface Sci.* **1999**, *218*, 397.
(33) Bustamante, C.; Tinoco, I., Jr.; Maestre, M. F. *Proc. Natl. Acad. Sci. U.S.A.* **1983**, *80*, 3568.
(34) Chaffotte, A. F.; Guillon, Y.; Goldberg, M. E. *Biochemistry* **1992**, *31*, 9694.
(35) Lyon, C. E.; Suh, E-S; Dobson, C. M.; Hore P. J. *J. Am. Chem. Soc.* **2002**, *124*, 13018.
(36) Silverman, B. D. *Proteins, Struct., Funct., Genet.* **2003**, *53*, 880.
(37) Agarraberes, F. A.; Dice, J. F. *Biochim. Biophys. Acta, Biomembr.* **2001**, *1513*, 1.
(38) Sogami, M.; Era, S.; Koseki, T.; Nagai, N. *J. Pept. Res.* **1997**, *50*, 465.
(39) Hasted, J. B. *Aqueous Dielectrics*; Chapman & Hall: London, UK, 1973.
(40) Grosse, C.; Foster, K. R. *J. Phys. Chem.* **1987**, *91*, 3073.
(41) Grosse, C. *J. Phys. Chem.* **1988**, *92*, 3905.
(42) Barchini, R.; Pottel, R. *J. Phys. Chem.* **1994**, *98*, 7899.
(43) Lobo, V. M. M.; Quaresma, J. L. *Handbook of Electrolyte Solutions*; Physical Science Data Series 4, Elsevier: Amsterdam, 1989; p 61.
(44) Lai, J. R.; Fisk, J. D., Weisblum, B., Gellman, S. H. *J. Am. Chem. Soc.* **2004**, *126*, 10514.
(45) Paci, E.; Vendruscolo, M. *J. Phys.: Condensed Matter* **2005**, *17*, S1617.
(46) Lindberg, C.; Selenica, M. L.; Westlind-Danielsson, A.; Schultzberg, M. *J. Mol. Neurosci.* **2005**, *27*, 1.
(47) Zagol-Ikapitte, I.; Masterson, T. S.; Amarnath, V.; Montine, T. J.; Andreasson, K. I.; Boutaud, O.; Oates, J. A. *J. Neurochem.* **2005**, *94*, 1140.

BM060609D